

A Novel Algorithm to Select a Seed Point Automatically In Breast Ultrasound Image

S.Michahial^{1*}, B.A. Thomas² and S.Kiran³

¹Department of EIE, GSSSIETW, Mysuru - 570016, Karnataka, India; staffordm@gsss.edu.in

²Department of ECE, VVIET, Mysuru – 570028, Karnataka, India; binduvviet@gmail.com

³JSS Medical College and Hospital, Mysore – 570015, Karnataka, India; sudha7492@gmail.com

Abstract

In automatic segmentation of breast ultrasound images, seed point is to be selected automatically for contour evolution to proceed. The total computation task involved in the initialization of seed point, occupies most of the system time and resource. In this paper, the proposed method computes and identifies the seed point automatically by which automatic contour initialization is done. In pre-processing stage Improved SRAD filter is developed and method for selection of seed point automatically is based on the changes in gray level intensities or texture features, which serves as an initialization for level set segmentation. The seed point that is automatically plotted on to Ultrasound B-scan images also plotted on its corresponding elastogram pair. Proposed method is applied on to 50 US B scan images of benign solid mass, 80 malignant solid mass and 30 images of complex and simple cysts. For validation process, the seed point obtained by the approach mapped on the image pairs. The above approach shows us that the work presented will successfully and seed point using texture values of US B scan Images with an accuracy of 87%. With this proposed method the computational time and resource used for segmentation of Breast lesions will be minimized to maximum extent and is more accurate.

Keywords: Automatic Seed Point, ISRAD, Texture analysis, Ultrasound B Mode Images

1. Introduction

Cancer is a deadly disease among which Breast cancer is the common of all cancer in women and rare case can affect men too. At an average 12.3% of women are been diagnosed with breast cancer during their life time. According to the survey in men, new cases 1.3 out of 100,000 and women 120 out of 100,000, out of which death caused by breast cancer is 0.3 per 100,000 in men and 21.9 per 100,000. Indian scenario 1 out of 28 women develop breast cancer. The ratio is set as Urban: rural :: 1 in 22 women: 1 in 60, Just 2 year ago , 154,957 women were newly detected every year among which 70,218 women die cause of breast cancer. An Average age of the high risk group: in western it is 55-57 years; India 43-46¹. A year down the lane, it is estimated that there will be 1, 56,000 new cases of breast cancer among which 77,000 women

in India will die due to the disease. The gap only seems to be widening, which means, we need to work aggressively on early detection. The Table 1 below will give the information about the detection rate of breast cancer in USA when compared to India. (Sources: SEER Survival Monograph (NCI), 2014; Chopra, Cancer Institute Chennai, India, 2011).

Conclusion of this table is that. USA: 90% DCIS or early staged invasive disease at diagnosis. Where as in INDIA: 76% locally advanced or metastatic at diagnosis. Screening is single most important factor for better survival of patients¹. Mammography was the most effective modality used to detect breast cancer previously which offers an overall 20% reduction in women aged between 40 to 74. 15% reduction rate was found in women aged between 40 to 49. 22% reduction rate in women aged between 50 to 74. As many as 5 to 15% of breast cancers

*Author for correspondence

Table 1. Survival rate at different stages of Breast cancer

Stage	Extent	5 Year Survival	Distribution	
			USA	INDIA
0	Noninvasive	100%	16%	---
I	Early Stage disease	100%	40%	1%
II	Early Stage disease	86%	34%	23%
III	Locally Advanced	57%	6%	52%
IV	Metastatic Disease	20%	4%	24%

are not detected mammographically, this means a negative mammogram should not deter work-up of a clinically suspicious abnormality. Lesion pick up depends on adequacy of the imaging system and technical factors, Optimal positioning of the breast and breast density. An alternative to mammogram is ultrasound imaging which is used by every 1 out of 4 researchers. Breast Ultrasound (BUS) Imaging when compared to Mammography is more superior, in the facts: (1) mammography has radiations effects on the patients and also not safer for the radiologists in daily practice, were as Ultrasound examination is safer and convenient than mammography^{2,3}. US examination is safer and also cheaper than mammography, hence ultrasound is fit for common man and affordable for all class of people. (2) US imaging is faster and sensitive for detecting abnormality in dense and fatty breasts than mammography, hence good the detecting the abnormalities for women below 35 years of age. (3) False positive rate in mammography is high which can be a reason for unnecessary biopsies, but the accuracy rate of US imaging for breast is 96 100% in diagnosis of simple cysts. Mammogram in congestion with ultrasound will increase the accuracy to detect the abnormality present in the breast cancer. Studies have suggested that using ultrasound imaging leads to high accuracy for distinguishing malignant and benign which in turn gives us a better recognition rate for detecting of cancer in breast images. US imaging use for detecting abnormalities is better tool to help the radiologists to make their decision better or increase the accuracy rate in detecting abnormalities. Computer Aided Diagnosis system (CAD) helps radiologists to find the affected area and more information about the breast abnormalities CAD system has four stages as given below.

1.1 Image Preprocessing:

BUS imaging has major limitations with respect to low contrast and interference with speckle. Image preprocessing step is done to clean image by removing speckle

noise and enhancing the edge details, boundary, texture features without degrading the information content of an image.

1.2 Image Segmentation:

Region of interest will be defined, separation of the abnormal area in breast image from the background is an important task.

1.3 Feature Extraction and Selection:

Features play a vital role to distinguish between lesion/non-lesion or benign/malignant.

1.4 Classification:

On the basis of the features obtained they are classified in to following BIRADS⁴.

- a) 0: Need Additional Imaging
- b) 1: Negative
- c) 2: Benign found
- d) 3: Probably Benign Finding - Follow up after a short interval of time
- e) Suspicious Abnormality - Biopsy to be Considered
- f) Highly Suggestive of Malignancy Appropriate Action Should Be Taken
- g) Histologically proven malignancy.

Few Methods in literature for selecting a seed point automatically are reported previously for ultrasound echography images. A formulae to evaluate the seed point from set of randomly selected points. The point is selected which has the highest score. Another method reported in. Once preprocessing, morphological operations are done, a binary image is obtained, the sum of the row and column are computed. Seed point is selected or evaluated based on the row and column number with maximum sum. Yet another method of automatic seed point, spatial characteristics and texture features of breast lesions are considered for selection of seed point.

2. Proposed Methodology

2.1 Image Acquisition:

In the work proposed, 160 images are used out of which 50 are benign mass, 80 malignant mass and 30 are simple and complex cyst. Apart from these images 40 electrog-

raphy images are tested with this for the purpose of validation. The study made in this paper is a retrospective analysis of the images stored and no impact at all on clinical management of the patients. The images used for the study taken from JSS medical hospital with the suggestion given by the doctors, the patient's information are anonymous. The images are obtained using Philips system with high frequency linear VF 6 Mhz-3 MHz transducer.

2.2 Segmentation of Lesion:

The steps involved in segmentation of abnormal solid masses in Breast US images

- Preprocessing stage: Improved SRAD filter is proposed to reduce noise and speckle.
- Automatic seed point selection: To select the seed point, novel algorithm is proposed in this paper.
- Gray value thresholding is done on the preprocessed image to obtain a binary image.
- Compute or find the position of seed point inside the region of interest i.e. inside lesion and trace the initial contour around this computed seed point automatically.

Apply Level set method and chain-vase method to segment the abnormal area of lesion of breast.

Due to noise and speckle found in Ultrasound-B Mode and electrographic images degrades image quality. Noise filtering and edge enhancement is required to compute the seed point efficiently⁶. Noise filtering methods of BUS images have several fundamental requirements. 1) Filter should not alter any information contain regarding object boundary and its detailed structure. 2) It should clean the image by removing noise in homogeneous area. 3) It should enhance the morphological features by smoothing and sharpening discontinuities. The Speckle Reducing Anisotropic Diffusion (SRAD) filter proposed by Yongjian Yu and T. Scott Acton in 2002⁷ meet the fundamental requirements to remove the noise and enhance the quality of the image. In this paper Improved SRAD diffusion is proposed which is based on setting a diffusion coefficient in the diffusion equation by using frame Laplacian and frame gradient. ISRAD uses 2 methods namely 1) Lee diffusion⁸

2) frost diffusion⁸ which creates a more general approach and updated function for the output image, by extending the PDE for removing the speckle as given

inequation .SRAD is based on the anisotropic diffusion which is nonlinear method that exhibits diffusion in homogeneous region and inhibits diffusion at edges⁹.

2.3 Improved SRAD

SRAD is based on the anisotropic diffusion which is nonlinear method that exhibits diffusion in homogeneous region and inhibits diffusion at edges. The PDE is given as follows.

$$\frac{\delta I}{\delta t} = \text{div} [c(|\nabla I|)\nabla I] \quad (1)$$

$$I(t=0)=I_0$$

Where ∇ is a gradient operator, DIV is divergence operator, $||$ denotes magnitude, $c(x)$ diffusion coefficients, and I_0 is the initial image.

Given the intensity $I_0(x,y)$ having the continuous form of SRAD is given by

$$(\delta I(x, y; t))/\delta t = \text{div}[c(x, y; t)\nabla I(x, y; t)] \quad (2)$$

$$I(x,y;0)=I_0, (\delta I(x, y; t))/(\delta n) \cdot \vec{\delta n} = 0 \quad (3)$$

Where $\delta\Omega$ denotes border of Ω , $\vec{\delta n}$ denotes outer normal to $\delta\Omega$, s is ICOV. Form 1 and 2 equation we see that PDE lie in the choice of diffusion coefficient $c(x)$. The $c(x)$ is given by

$$c_d(x,y) = \exp\left(-\left[\frac{|\nabla I_d(x,y)|^2}{k}\right]\right) \quad (4)$$

$\nabla I_d(x,y)$ is directional derivative in direction d at location (x,y) , diffusion coefficient is a function of s given by

$$c(x,y;t) = 1 + \frac{1}{\left[s_0^2(t) \left(1 + s_0^2(t)\right)\right]} \left[s^2(x,y;t) - s_0^2(t)\right] \quad (5)$$

Where $s(x,y;t)$ is given by the equation

$$s(x,y;t) = \sqrt{\frac{\left[\left(\frac{1}{2}\right)\left(\frac{|\nabla I|}{I}\right)^2 - \left(\frac{1}{4^2}\right)\left(\frac{\nabla^2 I}{I}\right)\right]}{\left[1 + \left(\frac{1}{4}\right)\left(\frac{\nabla^2 I}{I}\right)\right]}} \quad (6)$$

$s_0(t)$ which is the speckle scale computed from homogeneous region is given by

$$s_0(t) = \sqrt{\frac{\text{var}(z(t))}{z(t)}} \quad (7)$$

Form the above set of equations we see that S is small, c is larger, and hence diffusion will be done in homoge-

neous region and inhabited at the edges in SARD. One of the important steps of the SRAD filter is the choice of the homogeneous region to compute so which will affects the diffusion result. Let

$$r(x,y;t) = \frac{s^2(x,y;t) - s_0^2(t)}{s_0^2(t)} \tag{8}$$

and

$$S(t) = 1 + s_0^2(t) \tag{9}$$

Hence $c(x,y;t)$ can be expressed as

$$c(x,y;t) = \frac{1}{1 + \frac{r(x,y;t)}{S(t)}} \tag{10}$$

$r(x,y;t)$ is the one which effects the diffusion^{11,12} and $S(t)$ is used to normalize $r(x,y;t)$ to range [-1, 1] and when $s(x,y;t) = s_0^2(t)$; $c(x,y;t) = 1$; when $s(x,y;t) < s_0^2(t)$;

$c(x,y;t) > 1$; $s(x,y;t) > s_0^2(t)$; $c(x,y;t) < 1$; from this we conclude that $c(x,y;t)$ is the speed of diffusion. This means that the speed of diffusion will vary from region to region, which is different from conventional SRAD. If $s(x,y;t) = s_0^2(t)$ then diffusion is moderate, if $s(x,y;t) < s_0^2(t)$ then diffusion is faster and if $s(x,y;t) > s_0^2(t)$ then diffusion rate is slow. Hence $s_0^2(t)$ provides an initial reference point for diffusion. To make the selection of $s_0^2(t)$ automatic we replace the $s_0^2(t)$ with mean of $s_0(x,y;t)$ and the $c(x,y;t)$ is updated as

$$c(x,y;t) = \frac{1}{1 + \frac{[s^2(x,y;t) - s_0^2(t)]}{[s_0^2(1 + s_0^2(t))]} \tag{11}$$

$$\text{Where } s_0(t) = \lambda \iint_A s^2(x,y;t) dx \frac{dy}{\iint_A dx dy}$$

Where λ is the diffusion control parameter, A is the image domain. If we preserve edges a suitable λ must be selected which allows the diffusion to be carried out as follows. Contrast of region larger than average contrast, diffusion will be slower; Contrast of region smaller than average contrast, diffusion will be faster; diffusion is moderate in the region with similar contrast that of average contrasts. Hence

New Improved algorithm is better than using existing SRAD^{5,10}.

Active contour is the robust method generally used for segmentation. In this paper level set active contour

method used is based on 2nd criteria is used for segmentation, which is more robust than the original Osher and Sethian presented⁹.

2.4 Automatic Seed Point Selection

The intensity information is obtained from the gray level on an ultrasound image. The fat tissue relative to surrounding glandular tissue is hypoechoic. The glandular parenchyma tissue is homogeneously echogenic when compared to fat lobules. Cysts are usually anechoic. Malignant solid mass are hypoechoic, heterogeneous and appear black compared to surrounding fat. Benign solid masses imaged using ultrasound appears with uniform and intense hyper echogenicity. Texture features represent change in intensities¹⁴.

In our work the texture features calculated are energy, entropy, long run emphasis, Run Length Nonuniformity and Short Run Emphasis are calculated using the given in equations (12- 16) and are used to find the seed point automatically.

$$\text{Energy} = \sum_i^n \sum_j^n (p(i,j))^2 \tag{12}$$

$$\text{Entropy} = - \sum_i^n \sum_j^n P(i,j) \log_2(p(i,j)) \tag{13}$$

n is the number of gray level in image, $p(i,j)$ in a fixed size spatial window represents co-occurring probabilities of all pair wise combinations of gray level.

$$\text{Long run emphasis} = \frac{\sum_i^G \sum_j^R p(i,j)^2}{\sum_i^G \sum_j^R p(i,j)} \tag{14}$$

$$\text{Run length Nonuniformity} = \frac{\sum_i^G \sum_j^R p(i,j)^2}{\sum_i^G \sum_j^R p(i,j)} \tag{15}$$

$$\text{Short Run emphasis} = \frac{\sum_i^G \sum_j^R \frac{p(i,j)}{j^2}}{\sum_i^G \sum_j^R p(i,j)} \tag{16}$$

In Table 2 one the column represents the range of texture features for each of the abnormality listed in row for Breast ultrasound image.

The steps involved for seed selection is as given below. An image block is considered as shown in Fig 1. The center image block is (x,y) and its neighboring image blocks are $(x+1, y)$; $(x+2, y)$; $(x, y+1)$; $(x,y+2)$; $(x-1, y)$; $(x-2, y)$; $(x, y-1)$ and $(x, y-2)$ Workflow is given as

Work flow is given as

Table 2. Energy, entropy, short run emphasis (SRE) and run length nonuniformity (RLN), long run emphasis (LRE) within lesion area

Type of lesion	RLN	LRE	SRE	Energy	Entropy	Criterion
Malignant solid mass	38-65	<3	<0.9	.05-0.11	0.25-0.45	Energy < 0.1; entropy < 0.5 RLN > 40; LRE < 3; SRE < 0.9 or RLN > 5; LRE < 25; SRE < 0.9
Benign solid mass	38-65	<3	<0.9	0.04-0.21	0.25-0.58	Energy < 0.1; entropy < 0.5 RLN > 40; LRE < 3; SRE < 0.9 or RLN > 5; LRE < 25; SRE < 0.9
Simple Cyst	Gray run length matrix = 0			0.85-1.00	0.12-0.27	Energy > 0.95; entropy < 0.15

1. The Image of size (MxN) is processed by the ISARD filter to enhance its feature.
2. The image obtained after filtering is windowed in to a block of size (n x n).
3. Energy and entropy features are calculated for each of the block and as per criterion given in the Table 2 are considered for seed selection.
4. Now each of these image block is considered as reference block. 2 image block on top, left, right and bottom are checked for the same as step 3.
5. Step 4 is done until the entire image block as taken as reference point in the image.
6. Long run emphasis, Run Length Nonuniformity and Short Run Emphasis is calculated for the blocks repeated while moving from one reference point to next.
7. The median position is calculated and considers as seed point.

As seen in figure 2 and 3. Image block considered is 10x10 window. The row is considered as layers of breast tissue and segments as column. As seen in figure 2 and 3 there is no much difference in the value of energy and

entropy calculated for background tissue and lesion area of malignant mass. Similarly no difference in energy and entropy values calculated for benign solid mass and background tissue, background tissue and complex cyst is also similar to above case. From this we can conclude that just energy and entropy is not sufficient for calculating seed point. To achieve a better seed point selection, in addition to the energy and entropy features in our paper, long run emphasis, Run Length Nonuniformity and Short Run Emphasis are considered. As shown in figure 4 and 5, energy and entropy differ between background and lesion regions which are suitable for seed point selection.

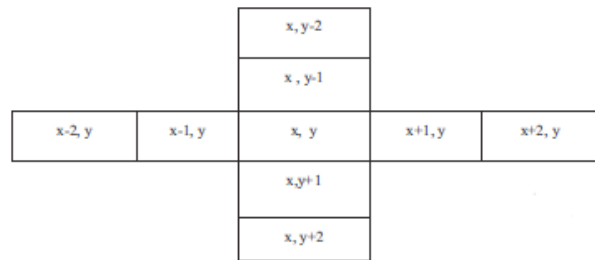


Figure 1. An image block and its neighbouring blocks

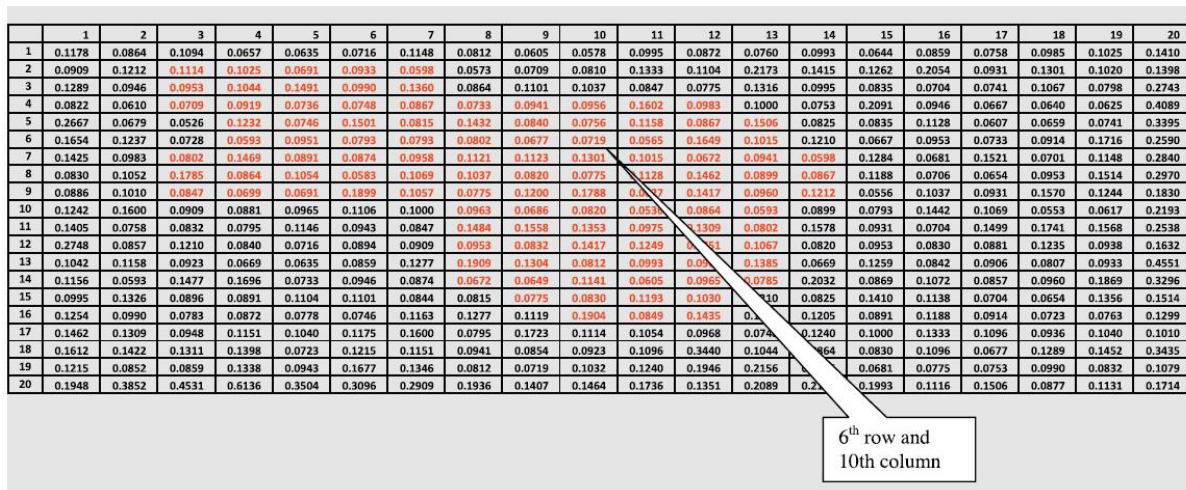


Figure 2. Energy matrix of the ultrasound image of a malignant mass

	1	2	3	4	5	6	7	8	9	10	11	12	13	14	15	16	17	18	19	20
1	0.4980	0.4489	0.4980	0.4980	0.4980	0.3373	0.4980	0.3373	0.3373	0.3373	0.3373	0.3373	0.3373	0.3373	0.4980	0.3373	0.4489	0.3373	0.3955	0.4980
2	0.5436	0.3373	0.2730	0.3955	0.4489	0.4489	0.3373	0.3373	0.1161	0.1161	0.2730	0.3373	0.3373	0.4489	0.4489	0.4980	0.4980	0.4489	0.6620	0.6620
3	0.5859	0.2730	0.2730	0.3373	0.2730	0.4980	0.2730	0.3955	0.4489	0.2730	0.2730	0.2730	0.4489	0.3373	0.2730	0.3373	0.3373	0.3373	0.1161	0.5436
4	0.4980	0.3373	0.3373	0.1161	0.2730	0.2730	0.3373	0.4489	0.2730	0.5436	0.5436	0.3955	0.3955	0.3955	0.3373	0.3373	0.3373	0.3373	0.3373	0.5436
5	0.3955	0.1161	0.3373	0.3373	0.2730	0.3373	0.3373	0.2730	0.3373	0.2730	0.2730	0.2730	0.3373	0.4489	0.2730	0.3373	0.3955	0.3373	0.2730	0.5436
6	0.4980	0.3955	0.3373	0.3373	0.2730	0.3373	0.3373	0.2730	0.2730	0.2730	0.2730	0.3373	0.2730	0.1161	0.3373	0.3373	0.3373	0.2730	0.3373	0.6253
7	0.3955	0.3373	0.2730	0.3373	0.3373	0.3373	0.2006	0.2730	0.3373	0.3373	0.3373	0.2006	0.4489	0.3373	0.2730	0.3373	0.1161	0.2730	0.2730	0.5859
8	0.3373	0.3955	0.2730	0.2730	0.2730	0.3373	0.3373	0.2730	0.2730	0.3955	0.3955	0.3373	0.3955	0.4489	0.3373	0.2730	0.1161	0.3373	0.3955	0.4980
9	0.3955	0.3955	0.4489	0.3373	0.3373	0.3373	0.2730	0.2730	0.2730	0.1161	0.1161	0.2730	0.4980	0.3373	0.1161	0.3373	0.2006	0.3373	0.3373	0.5859
10	0.3955	0.3955	0.3955	0.2730	0.2730	0.2730	0.2730	0.2730	0.2730	0.1161	0.2730	0.3373	0.3373	0.2730	0.3955	0.3373	0.4489	0.1161	0.3373	0.5436
11	0.4489	0.2730	0.2730	0.2730	0.3373	0.4980	0.2730	0.3373	0.3373	0.3955	0.2730	0.3373	0.1161	0.3373	0.5436	0.3373	0.2730	0.4489	0.3373	0.4980
12	0.3373	0.1161	0.1161	0.3955	0.2730	0.4489	0.3373	0.4489	0.4489	0.2730	0.2730	0.3373	0.3373	0.3373	0.3955	0.2006	0.3373	0.2730	0.3955	0.4980
13	0.4489	0.3955	0.4489	0.2730	0.1161	0.5436	0.4489	0.4489	0.4489	0.2730	0.2006	0.3373	0.2730	0.4489	0.3955	0.3955	0.3373	0.4489	0.3955	0.5859
14	0.3955	0.3373	0.3373	0.2730	0.3373	0.3373	0.3955	0.2730	0.3373	0.2730	0.3373	0.2730	0.3373	0.2730	0.1161	0.4489	0.4489	0.2730	0.2730	0.4489
15	0.3955	0.3955	0.4489	0.4980	0.4489	0.3373	0.3373	0.3373	0.3373	0.2730	0.3373	0.2730	0.3955	0.4980	0.3373	0.2730	0.1161	0.3373	0.2730	0.3373
16	0.5436	0.3955	0.3373	0.2730	0.3373	0.3373	0.3373	0.3373	0.4489	0.4980	0.4980	0.3955	0.3955	0.3373	0.4489	0.3373	0.2730	0.3373	0.2730	0.3373
17	0.3955	0.2730	0.2730	0.3373	0.3955	0.2730	0.2730	0.3955	0.2730	0.4489	0.4489	0.2730	0.3373	0.3955	0.3373	0.2730	0.2006	0.2730	0.2730	0.4489
18	0.4980	0.4489	0.3955	0.3373	0.2730	0.3373	0.3373	0.4980	0.3373	0.4980	0.2730	0.3373	0.3955	0.4489	0.4489	0.2730	0.2730	0.2730	0.3373	0.3955
19	0.3955	0.3955	0.3955	0.2730	0.4489	0.2730	0.3373	0.2730	0.3373	0.1161	0.3373	0.2730	0.3955	0.3373	0.2730	0.2730	0.3373	0.2730	0.3373	0.3373
20	0.5436	0.5436	0.6962	0.6962	0.6620	0.7281	0.5859	0.6253	0.4489	0.4489	0.3955	0.5859	0.5859	0.5859	0.3955	0.4489	0.4489	0.4980	0.3373	0.3955

Figure 3. Entropy matrix of the ultrasound image of a malignant mass.

	1	2	3	4	5	6	7	8	9	10	11	12	13	14	15	16	17	18	19	20
1	0.225	0.202	0.150	0.174	0.215	0.343	0.242	0.361	0.232	0.169	0.256	0.202	0.160	0.205	0.193	0.285	0.317	0.359	0.243	0.118
2	0.260	0.118	0.174	0.116	0.176	0.141	0.074	0.131	0.069	0.156	0.377	0.322	0.320	0.136	0.142	0.111	0.108	0.129	0.083	0.145
3	0.567	0.389	0.530	0.560	0.236	1.000	0.458	0.580	1.000	1.000	1.000	1.000	1.000	0.796	0.193	0.098	0.114	0.165	0.125	0.234
4	0.614	1.000	1.000	1.000	1.000	1.000	1.000	1.000	1.000	1.000	1.000	1.000	1.000	1.000	1.000	1.000	0.194	0.079	0.091	0.131
5	0.634	0.455	0.643	0.468	0.559	0.441	0.427	0.442	0.484	0.416	0.666	0.531	0.504	0.578	0.490	0.398	0.232	0.093	0.298	0.160
6	0.347	0.532	0.501	0.500	0.501	0.645	0.615	0.698	0.630	0.598	0.615	0.471	0.520	0.500	0.596	0.560	0.252	0.873	0.721	0.252
7	0.596	1.000	1.000	1.000	1.000	1.000	1.000	1.000	1.000	1.000	1.000	1.000	1.000	0.773	0.188	0.244	0.251	0.208	0.185	0.177
8	0.648	0.873	1.000	1.000	1.000	1.000	1.000	1.000	1.000	1.000	1.000	0.935	0.455	0.186	0.077	0.111	0.076	0.126	0.080	0.221
9	0.309	0.682	0.935	1.000	1.000	1.000	1.000	1.000	1.000	1.000	1.000	0.793	0.114	0.086	0.081	0.229	0.219	0.193	0.279	0.375
10	0.270	0.099	0.500	0.956	1.000	1.000	1.000	1.000	1.000	0.978	0.699	0.113	0.168	0.098	0.080	0.128	0.078	0.169	0.339	0.384
11	0.266	0.093	0.125	0.285	0.429	0.602	0.774	0.852	0.893	0.877	0.081	0.129	0.076	0.171	0.091	0.122	0.187	0.072	0.161	0.359
12	0.277	0.078	0.118	0.116	0.097	0.238	0.250	0.342	0.187	0.111	0.139	0.085	0.125	0.101	0.086	0.188	0.169	0.334	0.160	0.198
13	0.283	0.082	0.128	0.099	0.126	0.179	0.146	0.149	0.114	0.132	0.082	0.082	0.099	0.095	0.090	0.110	0.104	0.199	0.176	0.127
14	0.233	0.100	0.143	0.096	0.100	0.115	0.085	0.126	0.096	0.115	0.160	0.073	0.098	0.081	0.202	0.081	0.077	0.111	0.124	0.124
15	0.422	0.078	0.122	0.124	0.085	0.087	0.107	0.131	0.115	0.105	0.111	0.098	0.092	0.109	0.158	0.134	0.079	0.090	0.103	0.135
16	0.633	0.116	0.084	0.091	0.104	0.131	0.110	0.110	0.114	0.104	0.079	0.117	0.117	0.087	0.089	0.078	0.134	0.089	0.175	0.204
17	0.649	0.081	0.100	0.086	0.070	0.085	0.097	0.139	0.098	0.142	0.091	0.132	0.132	0.169	0.108	0.089	0.189	0.094	0.146	0.128
18	0.631	0.137	0.076	0.108	0.112	0.117	0.127	0.117	0.126	0.126	0.113	0.111	0.147	0.147	0.115	0.142	0.088	0.092	0.089	0.368
19	0.631	0.152	0.120	0.117	0.111	0.081	0.095	0.101	0.070	0.100	0.200	0.174	0.086	0.086	0.080	0.072	0.075	0.077	0.053	0.313
20	0.348	0.411	0.100	0.113	0.079	0.080	0.139	0.129	0.092	0.077	0.185	0.162	0.162	0.340	0.399	0.340	0.399	0.437	0.411	0.399

7th row and 8th column

Figure 4. Energy matrix of the simple cyst ultrasound image

	1	2	3	4	5	6	7	8	9	10	11	12	13	14	15	16	17	18	19	20
1	0.857	0.662	0.758	0.662	0.544	0.696	0.696	0.728	0.728	0.811	0.662	0.728	0.662	0.696	0.696	0.544	0.662	0.696	0.625	0.625
2	0.498	0.337	0.337	0.498	0.498	0.273	0.337	0.273	0.116	0.273	0.273	0.116	0.273	0.337	0.498	0.498	0.273	0.273	0.337	0.544
3	0.586	0.116	0.116	0.116	0.116	0.116	0.116	0.116	0.116	0.116	0.116	0.116	0.116	0.116	0.116	0.116	0.396	0.498	0.396	0.696
4	0.625	0.116	0.116	0.116	0.116	0.116	0.116	0.116	0.116	0.116	0.116	0.116	0.116	0.116	0.116	0.116	0.396	0.498	0.396	0.811
5	0.498	0.116	0.116	0.116	0.116	0.116	0.116	0.116	0.116	0.116	0.273	0.116	0.116	0.116	0.116	0.116	0.625	0.273	0.116	0.625
6	0.877	0.544	0.625	0.544	0.662	0.586	0.544	0.696	0.498	0.625	0.544	0.586	0.586	0.662	0.625	0.625	0.857	0.273	0.116	0.662
7	0.625	0.116	0.116	0.116	0.116	0.116	0.116	0.116	0.116	0.116	0.116	0.116	0.116	0.116	0.116	0.116	0.273	0.201	0.116	0.337
8	0.586	0.116	0.116	0.116	0.116	0.116	0.116	0.116	0.116	0.116	0.116	0.116	0.116	0.116	0.116	0.116	0.273	0.337	0.201	0.662
9	0.625	0.273	0.116	0.116	0.116	0.116	0.116	0.116	0.116	0.116	0.116	0.116	0.201	0.396	0.337	0.498	0.273	0.116	0.273	0.201
10	0.586	0.449	0.337	0.116	0.116	0.116	0.116	0.116	0.116	0.116	0.396	0.396	0.544	0.498	0.396	0.586	0.449	0.273	0.273	0.625
11	0.662	0.273	0.544	0.498	0.116	0.116	0.116	0.116	0.116	0.116	0.273	0.498	0.337	0.337	0.396	0.396	0.201	0.116	0.116	0.586
12	0.662	0.498	0.449	0.586	0.662	0.696	0.396	0.586	0.586	0.662	0.498	0.449	0.396	0.449	0.449	0.337	0.116	0.273	0.337	0.662
13	0.586	0.498	0.273	0.273	0.337	0.396	0.449	0.498	0.273	0.337	0.337	0.273	0.273	0.396	0.337	0.337	0.396	0.396	0.498	0.786
14	0.728	0.396	0.396																	

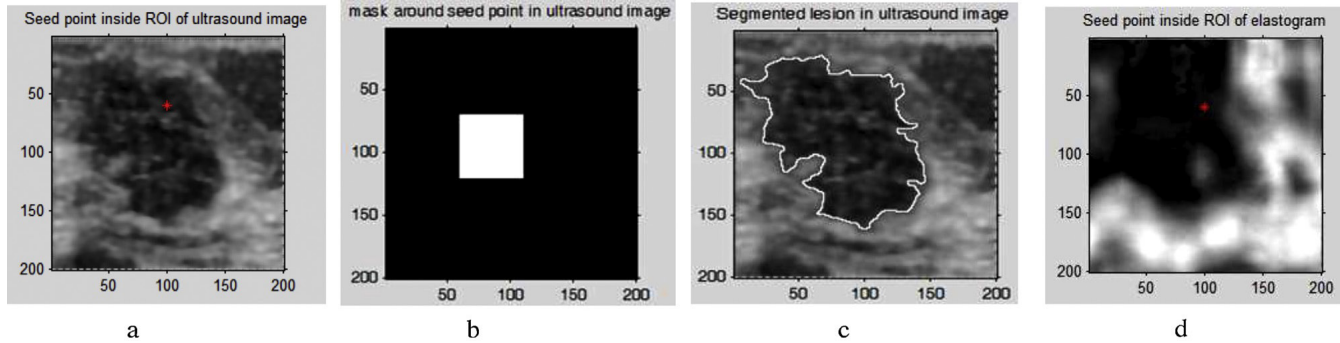


Figure 6 (a) Seed point plotted inside lesion area in US image of a malignant solid mass. (b) A mask for initialization around seed point. (c) Segmented lesion area in US image. (d) Seed point plotted inside lesion area of corresponding elastogram.

Lesion type	Total number of lesions	Number of lesions in which seed point is correctly detected	Accuracy
Benign solid mass	52	46	86.93
Malignant solid mass	84	72	
Cyst	63	55	

Figure 7. Performance analysis.

Region based level set method is used for segmentation using the seed point calculated from the proposed method by minimizing the Energy. In Level set method segmentation accuracy depends on the initial contour which in turn depends on the proper seed selection^{10, 13}. The above result is obtained for image obtained by using Philips Ultrasound imaging. “Region based level set method” does not use and gradient information. But separates the image into different regions based on the intensities. An Image $I(x,y)$ defined on Ω is assumed to be composed of 2 regions with homogeneous intensities with c_0 and c_1 . Let C be a curve that defines the boundary inside the region of Image $I(x,y)$. Homogeneity function is given by

$$E(c) = \int_{c \text{ inside}} |I - c_0|^2 d\Omega + \int_{c \text{ outside}} |I - c_1|^2 d\Omega$$

Where c_0, c_1 are average intensities value inside and outside the curve C . energy information is given by $E(c)$. , Image plane Ω can be segmented by local minimization of energy function. The idea is to evolve the boundary C from given region or point or Initialization in direction of negative energy gradient. In level set method most of the resources are wasted in order to find the initial contour which has to be automatically computed efficiently. In most of the previous work done in the literature the

contour are selected manually for segmentation or initial seed point is selected. In the present paper automatic seed point selection is done based on the texture features which are a base for level set to segment the breast lesion in an ultrasound image.

3. Results and discussion

Orderliness is represented in an image by energy i.e. the uniformity of intensity distribution. Energy range of malignant mass lies between 0.07 to 0.19 as shown in Fig 2. Energy range of a benign mass lies between 0.07 to 0.3. Energy range of a simple cyst lies between 0.4 to 0.1. Energy range of a complex cyst lies between 0.09 to 0.18.

Disorderliness is represented in an image by entropy i.e. the randomness of intensity distribution. Entropy is zero for smooth image. Entropy range of malignant mass lies between 0.27 to 0.49 as shown in Fig 3, Energy range of benign mass lies between 0.116 to 0.49, image block in simple cyst have value of entropy of 0.116. The gray run length, long run emphasis (LRE) is dependent on occurrence of long runs. Long run emphasis range from 1.21 to 50. Malignant solid mass and benign mass have a long run emphasis less than 3. The run length nonuniformity is a feature parameter that measures the similarity of length of runs through the image. It is assumed to be small if run length is similar through. RLN ranges from 18 to 81 for BUS images. Image block with malignant/benign solid mass will range from 38 to 65.

Simple Cyst Solid mass is marked as red star in figure 6a. The corresponding seed point block is shown in figure 2 with a call out. Mask is developed around the seed point as seen in figure 6b which serves as initial contour for level set. The automatic seed point selection algorithm proposed in this paper is applied on 160 images out of

which seed point accurately plotted in the lesion area is 142. The proposed method is 86.6% accurate. The performance of this algorithm is as shown in figure 7 for benign/malignant, cyst.

4. Conclusion

A novel approach for automatic seed point selection inside the breast lesion is proposed and hence to develop the initial contour around the seed point automatically. The proposed work is based on the variations in amplitudes of Echoes in the breast tissues. The variations correspond to change in intensity or gray level. Speckle, noise in the image is removed by the proposed ISRAD filter; divide the image in block of size 10x10 window; calculate the texture features energy and entropy and check for criterion of benign/malignant or simple or complex cyst; The gray run length, long run emphasis, short run emphasis, RLN features are found to accurately place the seed point in the lesion area of the breast ultrasound image. Initial contour is developed around the seed point and the lesion will be segmented using level set method. The proposed method is 86.6 % accurate and the approach is effective in selecting the seed point in lesion region automatically. Computation is easier and less time consuming.

5. References

1. Available from: <http://www.breastcancerindia.net/statistics/trends.html>.
2. Y.-L.Huang, Computer-aided diagnosis applied to 3-D US of solid breast nodules by using principal component analysis and image retrieval. Proceedings of the 2005 IEEE Engineering in Medicine and Biology 27th Annual Conference. 2005.p.1802-5.
3. Anderson B, Shyyan R, Eniu A, Smith R, Yip C. Breast cancer in limited resource countries: An overview of the breast health global initiative 2005 guidelines. The Breast Journal. 2006 Dec;S315.
4. Cosar ZS, Cetin M, Tepe TK, Cetin R, Zarali AC Concordance of mammographic classifications of micro calcifications in breast cancer diagnosis. Clinical Imaging. 2012 November; 389-95.
5. Michahial S, Bindu A Thomas BA, Comparison of Filters For Despeckle With Improved Speckle Reducing Antiscopic Diffusion Filter For Ultrasound Images. International Journal of Engineering Research in Electronic and Communication Engineering; 2016 May;3(5):461-7.
6. Yongjian Y, Scott TA. Speckle reducing anisotropic diffusion. IEEE Transactions on Image Processing. 2002.
7. Lee JS. Digital image enhancement and noise filtering by using local statistics. IEEE Transactions on Pattern Analysis and Machine Intelligence, PAMI-2: 1658 1980.
8. Frost VS, Stiles JA, Shanmugan KS, Holtzman JC. A model for radar images and its application to adaptive digital filtering of multiplicative noise. IEEE Transactions on Pattern Analysis and Machine Intelligence. 1982; PAMI-4:15765.
9. Osher S, Sethian JA. Fronts propagating with curvature-dependent speed: algorithms based on Hamilton-Jacobi formulations. Journal of Computational Physics. 1988; p:79:1249.
10. Michahial S, Thomas BA, Modified Level Set Method and Chain-Vese Methods using Srad Filter for Ultrasound Images. Elsevier proceeding. August 2014.
11. Sun Q, John A. Hossack, Tang J, Actonb ST. Speckle reducing anisotropic diffusion for 3D ultrasound images. Computerized Medical Imaging and Graphics. 2004:12.
12. Bini A. Despeckling low SNR, low contrast ultrasound images via anisotropic level set diffusion. Multidimensional Systems and Signal Processing. April 2012.
13. Shan, Juan, and Lin Li. A new scheme to evaluate the accuracy of knowledge representation in automated breast cancer diagnosis. 2014 International Conference on Collaboration Technologies and Systems (CTS). 2014.
14. Jaffar Baig MA, Thomas BA, Michahial S. Multiplicative Noise Reduction using Fuzzy Logic and Feature Analysis of Ultrasound Images. International Journal of Computer Application. Proceedings on NCESCO September 2015;(2):29-34.